Article

Title

Firstname Lastname [1,†,‡] [ID], **Firstname Lastname** [2,‡] **and Firstname Lastname** [2,*]

1   Affiliation 1; e-mail@e-mail.com
2   Affiliation 2; e-mail@e-mail.com
*   Correspondence: e-mail@e-mail.com; Tel.: (optional; include country code; if there are multiple corresponding authors, add author initials) +xx-xxxx-xxx-xxxx (F.L.)
†   Current address: Affiliation 3.
‡   These authors contributed equally to this work.

Abstract: A single paragraph of about 200 words maximum. For research articles, abstracts should give a pertinent overview of the work. We strongly encourage authors to use the following style of structured abstracts, but without headings: (1) Background: place the question addressed in a broad context and highlight the purpose of the study; (2) Methods: describe briefly the main methods or treatments applied; (3) Results: summarize the article's main findings; (4) Conclusions: indicate the main conclusions or interpretations. The abstract should be an objective representation of the article, it must not contain results which are not presented and substantiated in the main text and should not exaggerate the main conclusions.

Keywords: keyword 1; keyword 2; keyword 3 (List three to ten pertinent keywords specific to the article; yet reasonably common within the subject discipline.)

0. How to Use this Template

The template details the sections that can be used in a manuscript. Note that the order and names of article sections may differ from the requirements of the journal (e.g., the positioning of the Materials and Methods section). Please check the instructions on the authors' page of the journal to verify the correct order and names. For any questions, please contact the editorial office of the journal or support@mdpi.com. For LaTeX-related questions please contact latex@mdpi.com.

1. Introduction

Ultra-wideband (UWB) technology is a wireless communication protocol that enables short-distance communication through high-frequency radio waves. It first emerged in the 1970s in the United States and was initially developed for military applications such as radar and communication systems. Since then, military restrictions have been lifted, and commercialization began in the 2000s. However, UWB technology has not gained much attention due to its lower competitiveness compared to other wireless communication technologies such as WiFi and Bluetooth.

Nonetheless, the adoption of the High-Rate Pulse Repetition Frequency (HRP) and the establishment of the IEEE 802.15.4-2015 standard have helped to recognize the potential of UWB technology. UWB's ability to accurately determine location is due to its use of higher frequency bands than other wireless communication protocols. This feature is useful for indoor positioning systems, asset tracking, and other location-based services.

Furthermore, UWB technology has several advantages, including high data transfer speeds, low power consumption, and resistance to interference from other wireless signals. UWB signals are also difficult to intercept, making them a secure option for applications that require secure communication, such as payment systems and access control.

Overall, UWB technology has significant potential to transform the way we interact with technology and the world around us. Its accurate location sensing capabilities and high data transfer speeds make it a promising technology for a wide range of applications.

UWB technology has a bandwidth of up to 7.5 GHz, which allows it to achieve high-precision distance measurements with a resolution of several tens of centimeters using a short pulse width of 2 nanoseconds. By correlating UWB symbols, multiple channel impulse responses (CIRs) can be obtained, and by statistically analyzing the slight variations in these CIRs, a distance resolution of several centimeters or less can be achieved.

Recently, there have been advancements in implementing a direction-finding function using the PDoA (Phase Difference of Arrival) method. This involves analyzing the phase difference of CIRs received by multiple antennas. Additionally, the IEEE 802.15.4z-2020 standard includes an encryption function, which has been incorporated into many electronic devices.

Qorvo and NXP are the leading producers of Semiconductor ICs (Integrated Circuits) that use HRP UWB technology. These ICs are widely used in various fields, including automobiles and IoT devices, and are mounted on popular smartphones such as those from Apple and Samsung. The high-precision location sensing capabilities of UWB technology, including accurate direction and distance measurement, have enabled a range of applications, such as augmented reality (AR) technology and smart keys through encrypted communication.

One example of an application using UWB technology is the study of indoor occupancy, which can be used to determine the number of people in a given space. This technology is useful for improving building management, optimizing resource allocation, and enhancing safety and security in public places such as airports, shopping malls, and stadiums. Overall, the expanding range of applications using UWB technology is making it an increasingly important technology in various fields.

With the recent COVID-19 pandemic, it has become necessary to maintain a distance of at least 2 meters between people and limit the maximum number of people allowed indoors. Therefore, there is a growing need to introduce a system that can accurately identify and regulate the number of people in an indoor space.

Imaging technology has been traditionally used to determine the number of people indoors, but it can be challenging to accurately count the number of people in poorly lit areas or in places where people are partially obstructed by objects or other people. Similarly, using radar technology requires expensive high-output and high-performance radar systems, which are not price-competitive.

Alternatively, other communication technologies such as Bluetooth or WiFi can be used to determine the presence of people, but they are not effective in terms of accuracy, as they can only determine whether there is a person present or not. Thus, UWB technology, with its high-precision location sensing capabilities, offers a promising solution for accurately determining the number of people in indoor spaces, even in crowded and complex environments.

To address this problem, a research study was conducted on a system that uses UWB communication technology to accurately determine the number of people present in indoor spaces. Unlike Bluetooth or WiFi, UWB is less susceptible to data attenuation caused by the presence of multiple people or objects, due to its wider channel bandwidth and lower sensitivity to object interference. However, the CIR waveform of the UWB communication signal can still be affected by the surrounding environment and the number of people in the room.

By analyzing the CIR waveform, researchers were able to confirm that the waveform is formed differently depending on the number of people present in the room. Leveraging this knowledge, they developed a system that can identify the number of people present by analyzing the CIR waveform and using an artificial intelligence neural network to learn and distinguish the waveform pattern associated with different numbers of people. This system

could offer a practical and accurate solution to the challenge of regulating the number of people in indoor spaces during the current pandemic and beyond.

2. Experiment

2.1. Experiment environment setting

To collect data, we used Qorvo's DWM3000 module, which is the latest HRP UWB module supporting the IEEE 802.15.4z-2020 standard. This module allows for selective frequency channel settings based on domestic communication standards. For our experiment, we set the module to 9 channels as previously mentioned. To connect the module to the PC, we used Nordic's NRF-52840 microcontroller. We applied power and transmitted and received data through this setup.

As mentioned earlier, to obtain the CIR generated between transmission and reception between the two modules, the experimental environment was set up as follows. Firstly, for the Line of Sight (LoS) environment, the two modules were placed in a straight line, spaced 1m apart from the floor, and fixed using a tripod. Since the CIR is greatly influenced by the surrounding environment, efforts were made to create the same environment as much as possible, other than the variable for the number of people.

To conduct the experiment, continuous communication was established between the two UWB modules. The number of people in the environment was then varied from 0 to 5, and the corresponding CIR signals were measured. In total, 11 experiments were carried out. In each experiment, 500 CIRs were measured in a LoS environment without any people, and then the number of people was gradually increased up to 5, and an additional 500 CIRs were measured for each person. This resulted in a total of 6,000 CIRs per experiment, covering a range of 0 to 5 people.

To diversify the data, we varied the height, body shape, gender, and other factors for each person in the experiment. We also conducted the experiment in various environments to ensure data accuracy. Additionally, the data were acquired in two scenarios: when a person remained stationary and when a person moved and acted freely, in both static and dynamic states. For the human subjects, we selected adult males and females as our test subjects.

This is an example of a quote.

2.2. Experimental analysis of CIR

The UWB pulse width of 1nsec provides a distance resolution of 30cm, but it is possible to increase this resolution to several centimeters. This is achieved by transmitting UWB symbols repeatedly and detecting changes in CIR values through slight differences in the internal clocks of the hardware. The resulting CIR data contains 64 subtle differences, and a resolution of 1/64nsec is achieved through the use of the statistical data utilization algorithm LED (Leading Edge Detection). While the LED algorithm is not publicly disclosed as a unique patent of the UWB IC company, the CIR obtained through this method is provided as a parameter.
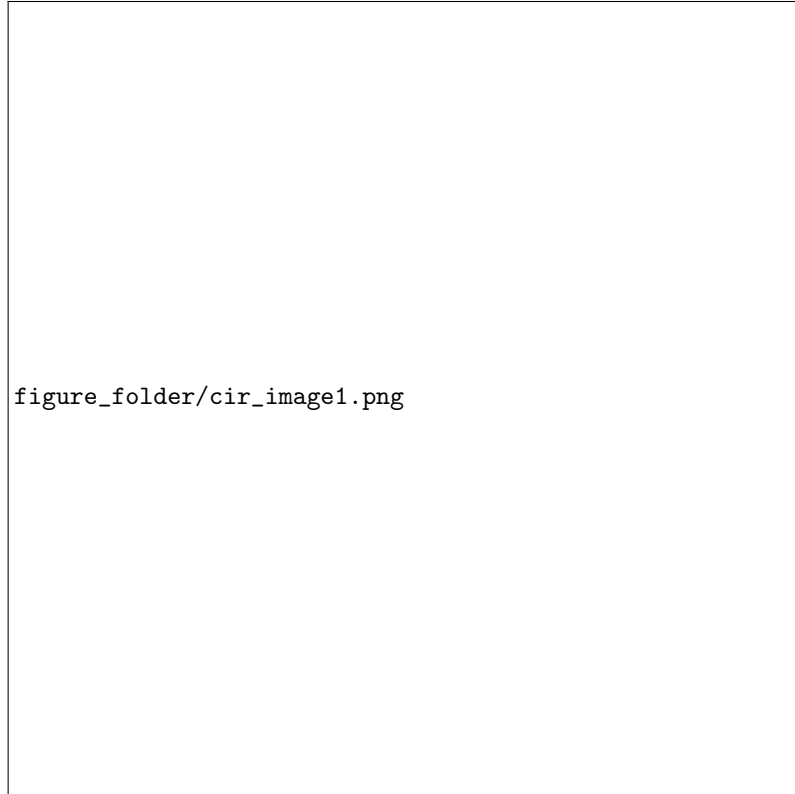
The first correlation point, which is the point that exceeds the threshold, among more than 1000 CIRs is called the FP_index, and 64 values can be obtained based on that point. Since the UWB receiver has an IQ demodulator structure, it obtains a Real CIR signal and an Imag CIR signal. If we convert that data into a series of vectors, we get:

$$RealCIR = [\alpha_1, \alpha_2, ..., \alpha_{64}], ImagCIR = [\beta_1, \beta_2, ..., \beta_{64}] \tag{1}$$

Using the two CIR signals and the formula below, Magnitude CIR and Phase, which represent the magnitude of the signal, can be obtained.
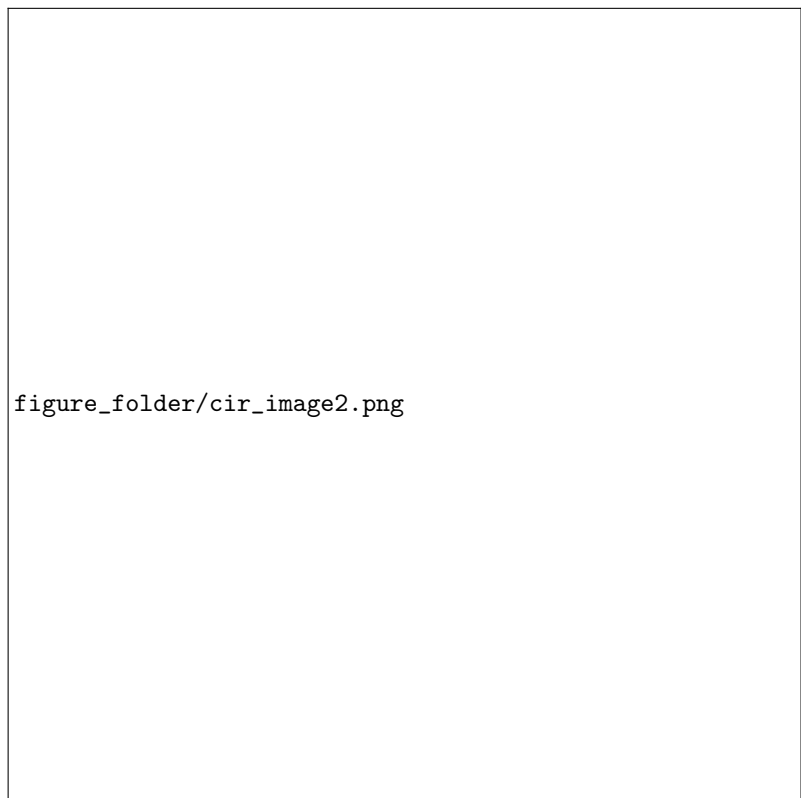
$$MagCIR = \sqrt{(RealCIR)^2 + (ImagCIR)^2}, Phase = arctan(Imag, Real) \tag{2}$$

We conducted a waveform comparison by dividing the dataset into two cases: static human channel impulse response (CIR) and dynamic human CIR. Firstly, we acquired a total of 12,000 human CIR signals in a static state, where the experiment was conducted with almost no positional changes within a 1-meter radius. As a result, we observed that reflected waves were generated due to people on the line of sight (LoS), and the dispersion increased as the number of people increased.

figure_folder/cir_image1.png

We also acquired 21,000 CIR signals while moving freely within a certain range on the LoS, and the resulting waveforms are as follows. It is evident that the CIR signal waveform in a dynamic state exhibits a smaller, noise-like waveform compared to the CIR signal in a static state, with the overall size generally being smaller. Furthermore, in both scenarios, it can be observed that the variance of the CIR waveform increases.

figure_folder/cir_image2.png

Prior to passing each raw data through the network, it is essential to normalize it to a range of 0 to 1 to reduce storage capacity requirements and improve memory processing speed. Normalization is achieved by applying the following formula, which utilizes the maximum and minimum values of each signal. This normalization process was executed using scikit-learn's library function.
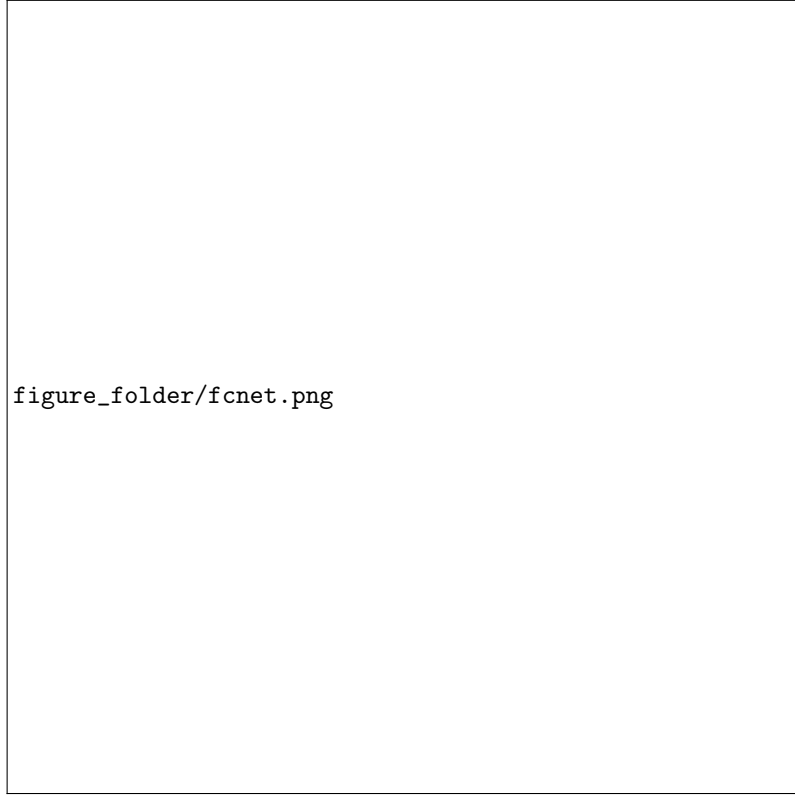
3. Network Implementation

3.1. Network Configuration

The Linux operating system served as the fundamental programming environment, while Python version 3.6.9 and Visual Studio Code were utilized for coding purposes. In configuring the network, tensorflow library version 2.3.0 was employed, with the ADAM optimizer utilized to train the network and minimize sparse categorical cross-entropy loss. Data pre-processing was performed using the sklearn library. To analyze the performance index, the entire dataset was divided equally into a train dataset (70%), a validation dataset (15%), and a test dataset (15%), segmented by class.

3.2. Fully Connected Layer

The initial network implemented is a Fully Connected Neural Network, where each feature vector is connected to all neurons. The network was configured based on the data obtained through experiments, with the number of parameters set manually. The figure below depicts a schematic diagram of the network.

```
figure_folder/fcnet.png
```

A single CIR generated in UWB produces 64 real and imaginary CIR values. These values are organized into a two-dimensional form of [2, 64] by stacking them.

$$CIR = [RealCIR, ImagCIR] \tag{3}$$

To simplify the operation, the corresponding input is transformed into a one-dimensional row vector using the flatten layer, which serves as the input layer. Upon passing through this initial input layer, the data is converted into 128 one-dimensional vectors.
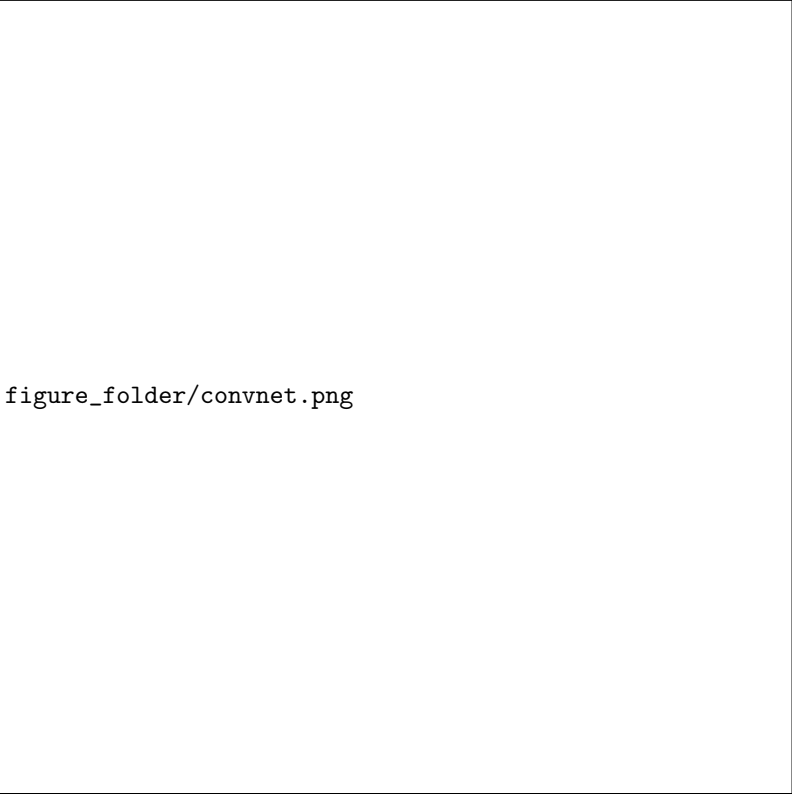
$$CIR = [RealCIR, ImagCIR] \tag{4}$$

The first hidden layer is a 2D array of [N, 128] consisting of parameter values and the size of the input layer.

The next output is obtained by performing a multiplication operation between the 2D array and the output of the input layer. The resulting expression is shown below.

$$CIR = [RealCIR, ImagCIR] \tag{5}$$

The resulting value obtained through this expression represents the output of the first hidden layer, with N parameter values. Similarly, the size and shape of the values are modified based on the parameter values of the subsequent layers. In the final output layer, the probability of the number of people is determined through the use of parameter 6 and the softmax function. The formula for calculating probability through the softmax function is presented below.

```
figure_folder/convnet.png
```

181

```
figure_folder/fullnetwork.png
```

182

4. Experiment Result

4.1. Fully Connected Style Network

Figure X (a) depicts the configuration of the FC Style Network. In order to compare accuracy, experiments were conducted by varying the number of hidden layers from 1 to 3, and setting parameter values between 16 and 1600. The table below presents the accuracy results based on the number of layers and parameter values.

183

184

185

186

187

188

Table 1. This is a table caption. Tables should be placed in the main text near to the first time they are cited.

Title 1	Title 2	Title 3
Entry 1	Data	Data
Entry 2	Data	Data [1]

[1] Tables may have a footer.

The accuracy generally increased as the number of layers increased. However, if the parameter value is set to its maximum, the network becomes overly complex, causing a slowdown in the calculation process, and ultimately leading to a decrease in accuracy. The complete results of the experiments can be found in the appendix.

4.2. Convolutional Style Network

Figure X (b) illustrates the configuration of the Convolutional Style Network. In the convolution layer, both the parameter values and the kernel size have an impact on the performance, so experiments were conducted by varying these two parameters as well as the number of layers. The parameter values were increased from 64 to 800, and the kernel size was increased from 3 to 15 in steps of 2. The accuracy results based on these parameters are presented in the table below.

Table 2. This is a table caption. Tables should be placed in the main text near to the first time they are cited.

Title 1	Title 2	Title 3
Entry 1	Data	Data
Entry 2	Data	Data [1]

[1] Tables may have a footer.

The accuracy of convolutional networks also tended to increase as the number of layers increased. Furthermore, the highest accuracy was achieved with appropriate parameter values and kernel sizes of 9 to 13. The complete experimental results can be found in the appendix.

4.3. Mix Style Network

The Mix Style Network was designed by connecting the Fully Connected Layer and the Convolution Layer. As shown in (c) of Figure X, the configuration consists of a convolution layer followed by one or two fully connected layers. The experiment was conducted with the parameter values of the convolutional neural network fixed at the highest performance. The results were compared by changing the kernel size of the convolutional layer, the number of subsequent fully connected layers, and the parameter values.

Table 3. This is a table caption. Tables should be placed in the main text near to the first time they are cited.

Title 1	Title 2	Title 3
Entry 1	Data	Data
Entry 2	Data	Data [1]

[1] Tables may have a footer.

The experiments were conducted with parameter values ranging from 16 to 4096 and with 1 or 2 fully connected layers. As with the previous experiments, parameter values that were too small were unable to contain all the necessary information for learning, and excessively large parameter values led to increased computation and reduced accuracy. The table below shows the accuracy according to the variables.

Overall, the Mix Style Network showed higher accuracy than the Fully Connected 216
Network, and comparable accuracy to the Convolutional Network. The optimal configura- 217
tion was found to be a convolutional layer with a kernel size of 11, followed by one fully 218
connected layer with 256 parameter values. All results of the experiment can be found in 219
the appendix. 220

4.4. AlexNet Style Network

Next, we constructed a network by adopting the AlexNet model designed for effective 222
image classification, which was presented at NIPS in 2012. We transformed the existing 223
2D network layer into a 1D form and conducted experiments by changing the parameters, 224
kernel size, and structure. The configuration diagram of the AlexNet Style Network is 225
shown in Figure X (d). 226

The AlexNet Style Network is composed of 5 Conv Layers and 2 FC Layers. In the 227
first Conv Layer, a wide range is brought in with a large kernel size, and after bringing a 228
narrow range of features through the next small kernel size, the FC layer learns informa- 229
tion. Between each layer, there is an operation to reduce or expand information through 230
MaxPooling Layer and ZeroPadding Layer. 231

Table 4. This is a table caption. Tables should be placed in the main text near to the first time they are cited.

Title 1	Title 2	Title 3
Entry 1	Data	Data
Entry 2	Data	Data [1]

[1] Tables may have a footer.

The accuracy was compared by changing the parameter value of the FC layer from 232
32 to 4096 while keeping the Conv layer fixed. However, as the layers deepened, the 233
time taken to train the model and the capacity of the model increased more than 10 times 234
compared to other models." 235

4.5. ResNet Style Network

Another network was constructed using the ResNet model, which was introduced 237
in 2015 for image learning. In a similar manner, a ResNet-style model was implemented 238
by converting existing 2D-type layers into 1D-type and incorporating skip connections. 239
Experiments were conducted by varying parameters, kernel size, and structure. The 240
structure of the ResNet Style Network is shown in Figure X(e). 241

In the case of the ResNet Style Network, block unit convolution is performed. Each 242
block consists of two Conv Layers, one BatchNorm Layer, and an Add Layer that adds the 243
existing values. A Conv Block is used when the existing size and the size created through 244
Conv are different, while an Identity Block is used when the sizes are the same. The block 245
diagram can be viewed in the figure below. 246

Table 5. This is a table caption. Tables should be placed in the main text near to the first time they are cited.

Title 1	Title 2	Title 3
Entry 1	Data	Data
Entry 2	Data	Data [1]

[1] Tables may have a footer.

blank 247

5. Additional Experiment

5.1. Hyperparameter Tuning

Hyperparameter tuning was performed based on the model with the highest performance in each network. First, an experiment was conducted by adding a norm layer between each layer, adding a dropout layer, and modifying the dropout rate. Afterwards, experiments were conducted with batch sizes of 16, 32, 64, 128, and 256. Finally, the learning rate was adjusted to bring out the optimal performance of the model. The table below shows the optimal performance for all models.

Table 6. This is a table caption. Tables should be placed in the main text near to the first time they are cited.

Title 1	Title 2	Title 3
Entry 1	Data	Data
Entry 2	Data	Data [1]

[1] Tables may have a footer.

Using the ResNet model, which had the highest performance through hyperparameter tuning, we checked the difference in accuracy by the number of people.

Table 7. This is a table caption. Tables should be placed in the main text near to the first time they are cited.

Title 1	Title 2	Title 3
Entry 1	Data	Data
Entry 2	Data	Data [1]

[1] Tables may have a footer.

5.2. Model Fusion

The model is known to create a different model each time, even under the same conditions with the same parameter values. To address this issue, models with similar performance were generated by adjusting the parameter values, and then fused to compare performance. By creating 3 to 4 models for each network and combining the evaluation of the TestSet, accuracy was improved.

Various fusion methods were attempted, including not only merging the same type of network but also combining different types of networks and using only the models with the highest performance.

Table 8. This is a table caption. Tables should be placed in the main text near to the first time they are cited.

Title 1	Title 2	Title 3
Entry 1	Data	Data
Entry 2	Data	Data [1]

[1] Tables may have a footer.

After evaluating the performance by fusing the models, it was found that the accuracy was improved by about 2 to 3% compared to using a single model. In particular, the FC model, Conv model, and ResNet model, which showed the highest performance, were selected, and their performance was checked. The result showed that the accuracy was about 86

5.3. Continuous CIR

To evaluate the performance of the model, CIR data was collected by acquiring 2 CIRs per second, and the number of people from 0 to 6 was detected. The existing evaluation

method only considered one CIR, but better performance could be achieved by considering multiple CIRs. The accuracy based on the number of CIRs is shown in the table below, which was tested using the ResNet Style Network with the highest performance.

Table 9. This is a table caption. Tables should be placed in the main text near to the first time they are cited.

Title 1	Title 2	Title 3
Entry 1	Data	Data
Entry 2	Data	Data [1]

[1] Tables may have a footer.

It was found that using two CIRs improved the accuracy by about 8-9%, and 100% accuracy was achieved when 10 CIRs were used. To obtain more detailed performance indicators, the error rate between the predicted and actual number of people was calculated using the Root Mean Square (RMS) method. Similar experiments were conducted based on the model with the highest performance in the ResNet Style Network.

Table 10. This is a table caption. Tables should be placed in the main text near to the first time they are cited.

Title 1	Title 2	Title 3
Entry 1	Data	Data
Entry 2	Data	Data [1]

[1] Tables may have a footer.

6. Conclusion

End

Bulleted lists look like this:

- First bullet;
- Second bullet;
- Third bullet.

Numbered lists can be added as follows:

1. First item;
2. Second item;
3. Third item.

The text continues here.

6.1. Figures, Tables and Schemes

All figures and tables should be cited in the main text as Figure 1, Table 11, etc.
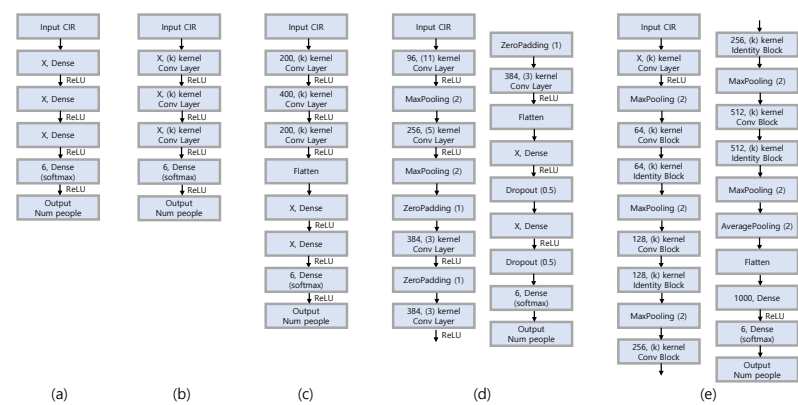
Figure 1. This is a figure. Schemes follow the same formatting. If there are multiple panels, they should be listed as: (**a**) Description of what is contained in the first panel. (**b**) Description of what is contained in the second panel. Figures should be placed in the main text near to the first time they are cited. A caption on a single line should be centered.

Table 11. This is a table caption. Tables should be placed in the main text near to the first time they are cited.

Title 1	Title 2	Title 3
Entry 1	Data	Data
Entry 2	Data	Data [1]

[1] Tables may have a footer.

The text continues here (Figure 2 and Table 12).

Figure 2. This is a wide figure.

Table 12. This is a wide table.

Title 1	Title 2	Title 3	Title 4
Entry 1 *	Data Data Data	Data Data Data	Data Data Data
Entry 2	Data Data Data	Data Data Data	Data Data Data
Entry 3	Data Data Data	Data Data Data	Data Data Data
Entry 4	Data Data Data	Data Data Data	Data Data Data

* Tables may have a footer.

Text.

Text.

6.2. Formatting of Mathematical Components

This is the example 1 of equation:

$$a = 1, \tag{6}$$

the text following an equation need not be a new paragraph. Please punctuate equations as regular text.

This is the example 2 of equation:

$$a = b + c + d + e + f + g + h + i + j + k + l + m + n + o + p + q + r + s + t + u + v + w + x + y + z \tag{7}$$

Please punctuate equations as regular text. Theorem-type environments (including propositions, lemmas, corollaries etc.) can be formatted as follows:

Theorem 1. *Example text of a theorem.*

The text continues here. Proofs must be formatted as follows:

Proof of Theorem 1. Text of the proof. Note that the phrase "of Theorem 1" is optional if it is clear which theorem is being referred to. □

The text continues here.

7. Discussion

Authors should discuss the results and how they can be interpreted from the perspective of previous studies and of the working hypotheses. The findings and their implications should be discussed in the broadest context possible. Future research directions may also be highlighted.

8. Conclusions

This section is not mandatory, but can be added to the manuscript if the discussion is unusually long or complex.

9. Patents

This section is not mandatory, but may be added if there are patents resulting from the work reported in this manuscript.

Abbreviations

The following abbreviations are used in this manuscript:

MDPI	Multidisciplinary Digital Publishing Institute
DOAJ	Directory of open access journals
TLA	Three letter acronym
LD	Linear dichroism

Appendix A

Appendix A.1

The appendix is an optional section that can contain details and data supplemental to the main text—for example, explanations of experimental details that would disrupt the flow of the main text but nonetheless remain crucial to understanding and reproducing the research shown; figures of replicates for experiments of which representative data are shown in the main text can be added here if brief, or as Supplementary Data. Mathematical proofs of results not central to the paper can be added as an appendix.

Table A1. This is a table caption.

Title 1	Title 2	Title 3
Entry 1	Data	Data
Entry 2	Data	Data

Appendix B

All appendix sections must be cited in the main text. In the appendices, Figures, Tables, etc. should be labeled, starting with "A"—e.g., Figure A1, Figure A2, etc.

References

1. Author 1, T. The title of the cited article. *Journal Abbreviation* **2008**, *10*, 142–149.
2. Author 2, L. The title of the cited contribution. In *The Book Title*; Editor 1, F., Editor 2, A., Eds.; Publishing House: City, Country, 2007; pp. 32–58.
3. Author 1, A.; Author 2, B. *Book Title*, 3rd ed.; Publisher: Publisher Location, Country, 2008; pp. 154–196.
4. Author 1, A.B.; Author 2, C. Title of Unpublished Work. *Abbreviated Journal Name* year, *phrase indicating stage of publication (submitted; accepted; in press)*.
5. Author 1, A.B. (University, City, State, Country); Author 2, C. (Institute, City, State, Country). Personal communication, 2012.
6. Author 1, A.B.; Author 2, C.D.; Author 3, E.F. Title of presentation. In Proceedings of the Name of the Conference, Location of Conference, Country, Date of Conference (Day Month Year); Abstract Number (optional), Pagination (optional).
7. Author 1, A.B. Title of Thesis. Level of Thesis, Degree-Granting University, Location of University, Date of Completion.
8. Title of Site. Available online: URL (accessed on Day Month Year).